

IMPERIAL COLLEGE LONDON
MSC MAJOR INDIVIDUAL PROJECT 2023-2024

Progress Report

Student:

Noah Saad (01905932)

Supervisor:

Dr Warren Macdonald

March 1, 2024

Word Count: 3257

**Imperial College
London**

Contents

| | |
|---|-----------|
| 1 Project Specification | 2 |
| 1.1 Introduction | 2 |
| 1.2 Aims of the Project | 2 |
| 1.3 Hypothesis | 2 |
| 2 Ethical Analysis | 3 |
| 3 Literature Review | 4 |
| 3.1 Current Key Findings | 4 |
| 3.2 Applications of Literature to Current Study | 6 |
| 3.2.1 Accurate Model of the Knee with Ligaments | 6 |
| 3.2.2 Accurate Model and Mechanical Properties of the Ligaments | 8 |
| 3.2.3 Accurate Kinematic Data of Computational Model | 9 |
| 3.2.4 Differential Intra-Bundle Strain (DIBS) | 9 |
| 4 Implementation Plan | 10 |
| 5 Risk Register | 11 |
| 6 Evaluation | 13 |
| 6.1 Measures of Success | 13 |
| 6.2 Potential Limitations | 13 |
| 7 Preliminary Results | 15 |
| 7.1 Computational Model | 15 |
| 7.2 Partial Validation of Model Kinematics | 16 |
| 7.3 Including External Force on the model | 17 |
| 7.4 Including Muscle Activation on the Model | 17 |
| 7.5 Procedure for Optimisation | 18 |
| 7.5.1 Scenario 1: Desired Joint Angle | 18 |
| 7.5.2 Scenario 2: Desired Torque | 19 |
| A Further Details Model | 23 |

1 Project Specification

1.1 Introduction

Anterior cruciate ligament (ACL) reconstruction surgery is one of the most common orthopaedic procedures performed each year. ACL injuries occur with increasing incidence, from approximately 33 cases in 100 000 in 1994 to between 40 and 60 incidents in 100 000 in 2014 [1]. The procedure consists in replacing the ruptured ACL by leveraging an arthroscopic intervention, removing the torn ligament, drilling tunnels from the original ACL footprints and passing a graft to replace it. Autogenous hamstring tendon (HT) and patellar tendon (PT) grafts are most commonly used for this purpose worldwide, at 63% and 26% respectively [2]. Currently, there is no standard procedure to determine the initial fixation strength of the new graft, and it is often left to the expertise of the surgeon [3]. While revision surgeries are minimal, improper graft tensioning may account for 77% of revision surgeries [4].

The optimum amount of force applied to the graft prior to fixation is a matter of considerable debate, with most authors recommending between 20 and 90 N of initial graft tension ([5],[6], [7]). Improper graft tensioning results in knee laxity or stiffness. The former can cause unnatural movements that can degrade the cartilage and contribute to osteoarthritis [8]. It was estimated that around 11% of patients go on to develop osteoarthritis (OA) as a consequence of unnatural joint mechanics incurred by inappropriately tensioned grafts.

On the other hand, over-tensioning the graft can over-constrain the knee potentially resulting in the loss of range of motion, an unfavourable environment for biologic incorporation and potentially graft failure ([9] [10]).

As such, it is worthy to investigate how the initial tensioning of the graft should change as a function of its stiffness.

1.2 Aims of the Project

The aim of the project are broken down into several smaller goals that will help achieve the main goal which is to **develop an accurate model of the knee joint to determine initial graft tensioning for ACL reconstruction surgery based on its stiffness**. The smaller goals that will aid in achieving the bigger one can be found below.

1. Create an accurate model of the knee joint including all the ligaments.
2. Mathematically describing the behaviour of the graft
3. Obtain stiffness data of grafts
4. Obtain a valid function or description of the movement to be tested
5. Predict the strain of the ACL during movement
6. Determine dangerous and unnatural movements
7. Analyse what the optimal tension should be as a function of graft stiffness

1.3 Hypothesis

It has been shown in numerous studies that tendon stiffness is extremely variable [11], as such it is hypothesised that the initial graft tension must be determined based on its stiffness to avoid over stiffening the joint (reducing the ROM) or causing unnatural movements that can contribute to the development of osteoarthritis.

2 Ethical Analysis

This research project addresses the crucial objective of establishing the initial graft tension of the ACL graft in ACLR. The computational model utilised in this study is constructed from cadaver data obtained from conducted studies.

It is of utter importance that the computational model correctly describes the motion of the knee and a rigorous validation procedure will be conducted to ensure that the model can be used to establish conclusions in the study. The validation can include comparison between all ligament strains at different knee flexion angles and collected data in the literature.

The project aims to refine the ACL reconstruction procedure, ensuring that patients can regain their pre-ACL tear functionality while minimising the risks of re-injury or the need for revision surgery.

The potential long-term impact of this project is profound. Successful integration of the proposed tension measurement step into ACL reconstruction has the potential to minimise revision surgeries and ACL graft failure.

Beyond medical implications, the project holds broader societal relevance by offering an improved standard of care for ACL reconstruction. The potential reduction in revision surgeries and associated healthcare costs could have positive economic implications. Furthermore, the environmentally conscious use of existing cadaver data aligns with sustainability goals in medical research.

In conclusion, this project's ethical foundation, reliance on validated data, and commitment to patient welfare underscores its potential significance in improving ACL reconstruction procedures. The long-term effects are poised to influence surgical practices, benefiting both patients and the broader medical community while maintaining ethical standards and minimising environmental impact.

3 Literature Review

3.1 Current Key Findings

Studies have demonstrated that initial graft fixation strength has a direct impact on knee biomechanics. Table 3.1, summarises these studies.

Table 3.1: Studies analysing the effect of initial graft tensioning in ACL reconstruction

| Authors | Title | Conclusion | Methods | Further research |
|------------------------------|--|--|---|--|
| Suggs et al (2003) [12] | The effect of graft stiffness on knee joint biomechanics after ACL reconstruction | "Graft stiffness has a direct impact on knee biomechanics after anterior cruciate ligament reconstruction." | 3D computational model | "Optimal anterior cruciate ligament reconstruction can be achieved if the anterior cruciate ligament is replaced by a graft with similar structural stiffness" |
| Arneja et al. (2009) [5] | Graft tensioning in anterior cruciate ligament reconstruction | There is a trend that suggests that 80 N of tension is the most effective amount of tension to apply during ACL reconstruction using hamstring-polyester graft sources. No conclusion for patellar graft. Unable to provide recommendations for tension to apply to 4-strand semitendinosus-gracilis autografts without polyester augmentation as no randomised clinical trial conducted | Systematic review of randomised controlled trials | Personalise initial tension magnitude based on properties of graft |
| Abramowitch et al (2003) [7] | The effect of initial graft tension on the biomechanical properties of a healing ACL replacement graft: a study in goats | "High initial graft tension could better replicate the normal knee kinematics at time-zero, however these effects may diminish during the early graft healing process." | Study in goats | Personalise graft tension based on graft material properties |

| | | | | |
|---------------------------|---|---|---|--|
| O'Neill et al (2011) [13] | Anterior cruciate ligament graft tensioning. Is the maximal sustained one-handed pull technique reproducible? | The maximal sustained one-handed pull technique of ACL graft tensioning is not reproducible from trial to trial. The initial tension placed on an ACL graft varies from surgeon to surgeon. | Device to simulate ACL reconstruction surgery using Ilizarov components and porcine flexor tendons. Six experienced ACL reconstruction surgeons volunteered to tension porcine grafts using the device to see if they could produce a consistent tension. | Graft tensioning needs to be considered and measured. One cannot rely on experience to tension effectively |
|---------------------------|---|---|---|--|

From table 3.1, it is clear that initial tensioning of the graft has an effect on the biomechanics of the knee following reconstruction. Additionally, it has been shown that surgeons cannot reproduce exact tensioning force. The main suggestion in these studies is that for optimal reconstruction, the graft tension must be appropriate for the individual and measured. It is now worthy to investigate whether the properties of the graft are patient-specific, if not, a general solution can be developed to tension all graft identically. Table 3.2 summarises the findings of variability between mechanical properties of grafts for ACL reconstruction. Furthermore, the method of fixation also modifies the stiffness of the graft. Common methods include Twisted and Parallel graft placement. These further amplify the differences between cases. These findings are also summarised in table 3.2.

Table 3.2: Summary of finding on variability of hamstring grafts for ACLR

| Authors | Title | Conclusion | Methods | Further research |
|--------------------------|--|--|---|---|
| Malige et al (2022) [11] | Biomechanical properties of common graft choices for anterior cruciate ligament reconstruction | Hamstring graft source maximum failure loads is extremely variable ranging from 225N to 4590N as can be seen in figure 3.1 | Systematic review that included twenty-six articles | - |
| Kim et al. (2003) [14] | Twisting and Braiding Reduces the Tensile Strength and Stiffness of Human Hamstring Tendon Grafts Used for Anterior Cruciate Ligament Reconstruction | Equally tensioned, parallel four-strand human hamstring tendon grafts were significantly stronger and stiffer than twisted or braided four-strand hamstring tendon grafts. | Paired <i>in vitro</i> biomechanical study. | Stiffness values of grafts need to be adjusted based on fixation method |

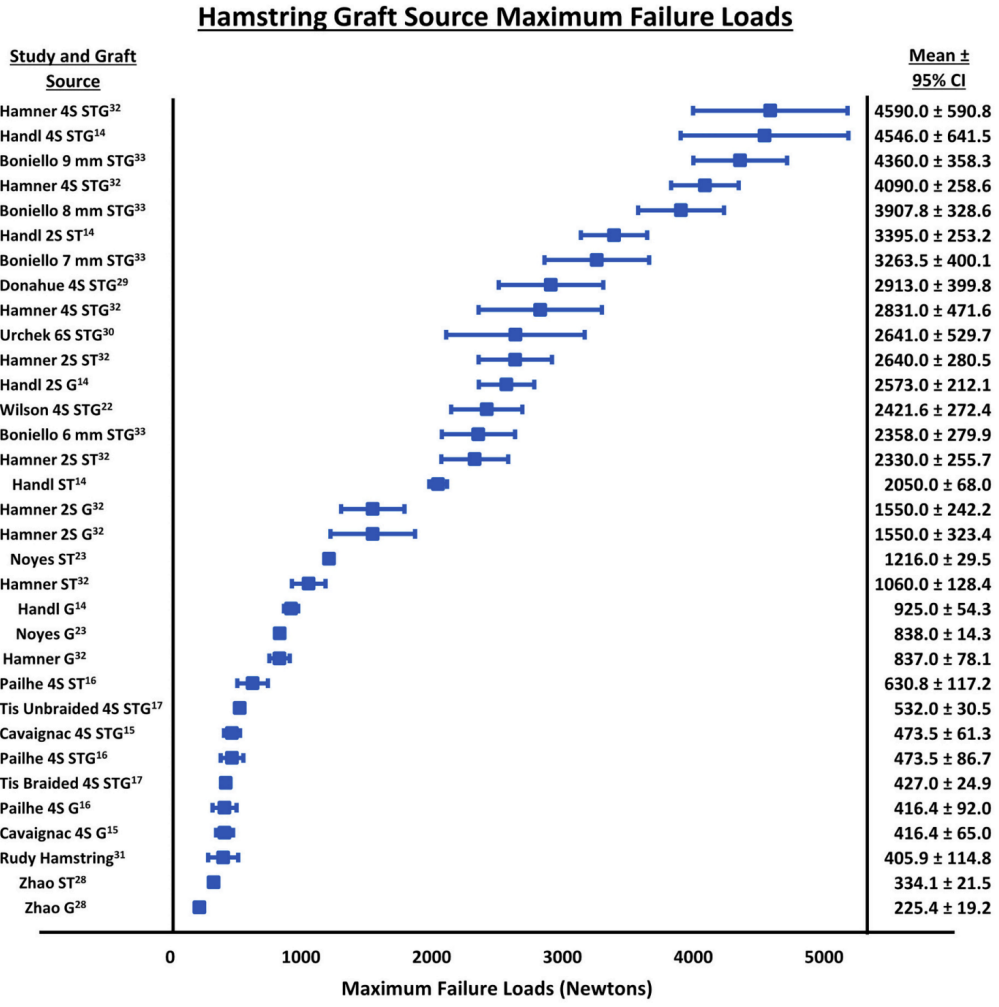


Figure 3.1: High variability in maximum failure loads for hamstring grafts [11]

It is therefore not allowed to assume that graft tensioning should be of the same magnitude for all patients undergoing ACLR and a personalised solution must be found in order to optimise recovery and reduce revision rates.

3.2 Applications of Literature to Current Study

This section summarises all methods and data utilised previously in the literature that will be applied in the current study. In order to build an accurate model, the ligaments must be placed anatomically correctly in the knee. Additionally, the ligament properties must match the literature. Finally, the model including the muscles and tendon must also be correct.

3.2.1 Accurate Model of the Knee with Ligaments

The study conducted by Xu et al. [15] provides an accurate model of the knee ligaments in OpenSim. The study used data collected by Blankevoort et al. [16]. Figure 3.2 shows the model including the knee ligaments. This computational model has been verified with cadaver data and can therefore be used in this study. The insertion sites of the ligaments can be found in table 3.3.

Table 3.3: Position of ligament insertion in body frame in cm. Data taken from Xu et al. [15]

| Ligament Name | X_{fem} | Y_{fem} | Z_{fem} | X_{tib} | Y_{tib} | Z_{tib} | Slack Length | Stiffness (N) |
|---------------|-----------|-----------|-----------|-----------|-----------|-----------|--------------|---------------|
| aACL | -0.718 | -40.037 | 0.407 | 1.657 | -3.009 | -0.074 | 3.23 | 1500 |
| pACL | -1.495 | -40.981 | 0.999 | 0.25 | -3.25 | 0 | 2.47 | 1600 |
| aPCL | -0.867 | -41.342 | -0.925 | -2.045 | -3.314 | 0.333 | 2.58 | 2600 |
| pPCL | -1.588 | -40.574 | -1.629 | -1.471 | -3.175 | -0.407 | 2.52 | 1900 |
| LCL | -0.978 | -40.056 | 3.45 | -0.71 | -6.056 | 3.725 | 5.59 | 2000 |
| aMCL | -0.741 | -40.435 | -3.5 | 0.768 | -7.96 | -2.762 | 7.22 | 2500 |
| iMCL | -1.274 | -40.62 | -3.351 | 0.249 | -8.256 | -2.91 | 7.31 | 3000 |
| pMCL | -1.777 | -40.361 | -3.351 | 0.249 | -9.403 | -2.64 | 8.8 | 2500 |
| aDMCL | -0.741 | -40.435 | -3.5 | 0.471 | -4.4 | -3.5 | 3.63 | 2000 |
| pDMCL | -1.777 | -40.361 | -3.351 | -0.5 | -4.4 | -3.5 | 3.72 | 4500 |

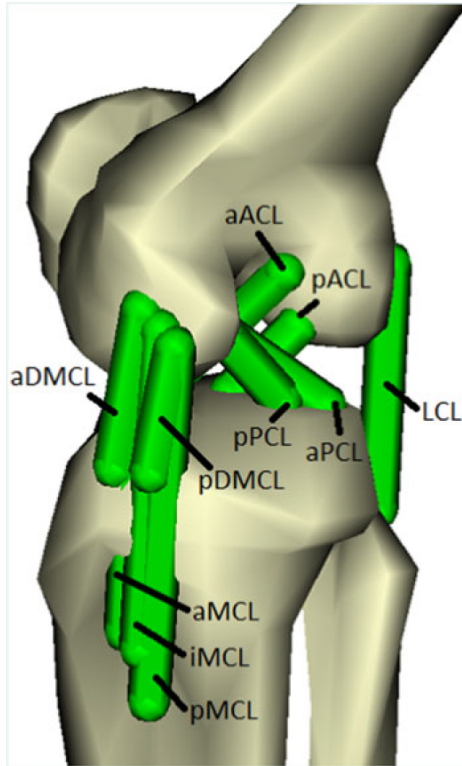


Figure 3.2: The abbreviations are: aACL, anterior bundle of the ACL; pACL, posterior bundle of the ACL; aPCL, anterior bundle of the PCL; pPCL, posterior bundle of the PCL; aMCL, anterior bundle of the superficial layer of the MCL; iMCL, inferior bundle of the superficial layer of the MCL; pMCL, posterior bundle of the superficial layer of the MCL; aDMCL, anterior bundle of the deep layer of the MCL; pDMCL, posterior bundle of the deep layer of the MCL [15]

3.2.2 Accurate Model and Mechanical Properties of the Ligaments

The ligament properties must also be in line with the literature. OSC models the ligament using the paper published by Blankevoort et al. [16]. The study obtained the kinematic data by using Roentgen Stereophotogrammetry (RSA). The model to be used can now accurately describe the kinematics of the knee ligaments. The mechanical properties of the ligaments will be taken from the study conducted by Xu et al. [15]. The properties are accurate and representative of the general population which is appropriate for the purpose of this study. The stiffness properties can be found in table 3.3. The kinematics and the force-strain curve are implemented into the computational model and can be found in the study by Blankevoort [16]. The ligaments are modelled as passive springs with the force-strain relationship described by a quadratic "toe" region, representing the uncrimping and alignment of collagen fibers, at low strains and a linear regions, representing the stretching of aligned collagen fibers, at high strains. The model incorporates a damping force, which becomes active solely when the ligament undergoes stretching beyond its slack length and is in the process of lengthening [17]. Figure 3.3 and the equations below describe the model.

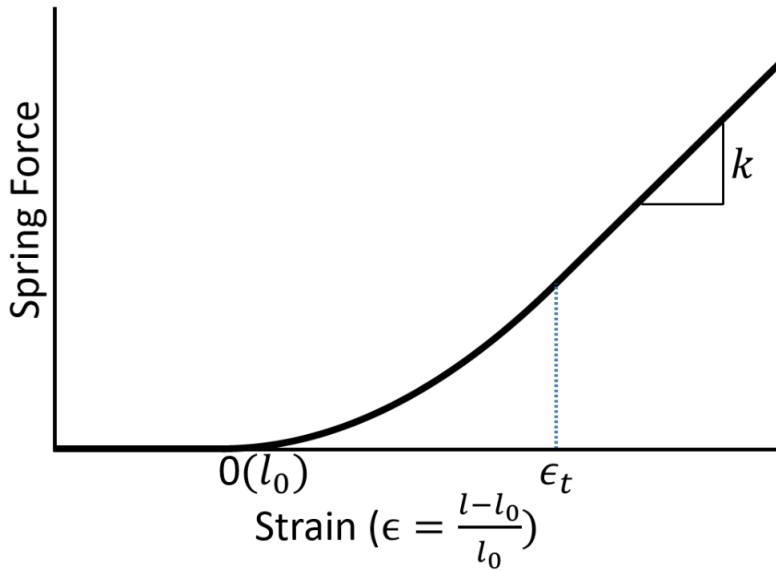


Figure 3.3: Stress-strain curve of Blankvoort Ligament [17]

$$F_{\text{spring}} = \begin{cases} 0, & \epsilon < 0 \\ \frac{1}{2\epsilon_t} k \epsilon^2, & 0 \leq \epsilon \leq \epsilon_t \\ k(\epsilon - \frac{\epsilon_t}{2}), & \epsilon > \epsilon_t \end{cases}$$

$$F_{\text{damping}} = \begin{cases} c \cdot \dot{\epsilon}, & \epsilon > 0 \text{ and } \dot{\epsilon} > 0 \\ 0, & \text{otherwise} \end{cases}$$

$$F_{\text{total}} = F_{\text{spring}} + F_{\text{damping}}$$

Where,

k is the slack length

ϵ is the strain

ϵ_t is the transition strain. The default value is 0.06 (6%) according to Blankevoort [16]. This value is widely used in the multibody knee modelling literature ([18], [19], [20], [21]) and also agrees with some experimental studies [22]. However, other literature suggests the transition strain of ligaments occurs at around 0.03 (3%) strain ([23], [24]). In reality, the transition strain is likely dependent on the strain rate ([25], [26]), however this effect is not included in this implementation.

$\dot{\epsilon}$ is the strain rate

c is the damping coefficient. Default is 0.03.

Note that the data for the ACL needs to be modified as the ligament is being replaced by the HT graft. It can be assumed that the tendon behaves similarly to the ligament as demonstrated by Kaya [27]. As such, only the stiffness of the tissue needs to be amended in line with the values found in the systematic review [11].

3.2.3 Accurate Kinematic Data of Computational Model

The model must be able to accurately represent the movement, strain and forces of the ligaments. The most important factor is the movement as the change in length as a result of the movement will be used to calculate the force generated by a ligament using the Blankevoort model [16]. The movement of the ligaments in the model will be compared with the study conducted by Xu et al. which verified the model using cadaver data [15]. The knee will be modelled at different flexion and internal/external rotation angles and the strains at these angles will be compared with the published study. Figure 3.4 shows an example of the strain of the LCL varies with respect to the internal/external rotation of the knee.

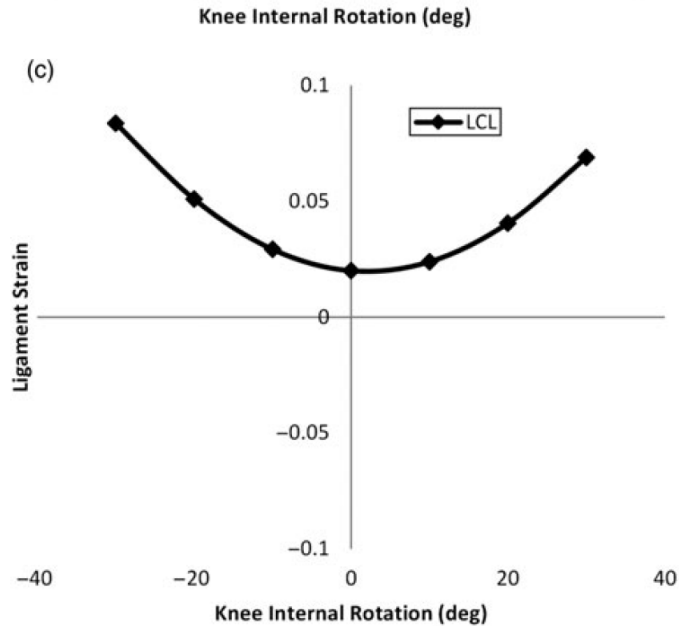


Figure 3.4: LCL strain with varying internal rotation angles of the knee [15]

3.2.4 Differential Intra-Bundle Strain (DIBS)

As we are modelling the ligaments of the same bundle as separate entities, it is necessary to be able to combine the strains in order to determine the total strain of the bundle. Marieswaran et al published the method known as the Differential Intra-Bundle Strain (DIBS) where ligaments of the same bundle can be combined to determine an overall strain [28]. The equation for DIBS is below.

$$DIBS_{i,j} = \begin{cases} |\epsilon_i - \epsilon_j|, & \epsilon_i, \epsilon_j \geq 0 \\ 0, & \epsilon_i, \epsilon_j \leq 0 \\ \begin{cases} 0, & (\epsilon_i + \epsilon_j) \leq 0, \\ |\epsilon_i + \epsilon_j|, & (\epsilon_i + \epsilon_j) > 0, \end{cases} & \forall(\epsilon_i < 0) \cap (\epsilon_j > 0) \end{cases}$$

Where ϵ_i is strain in the i th bundle and ϵ_j is strain in the j th bundle.

4 Implementation Plan

Figure 4.1 depicts a Gantt chart with all tasks that have been completed and those that have yet to be completed.

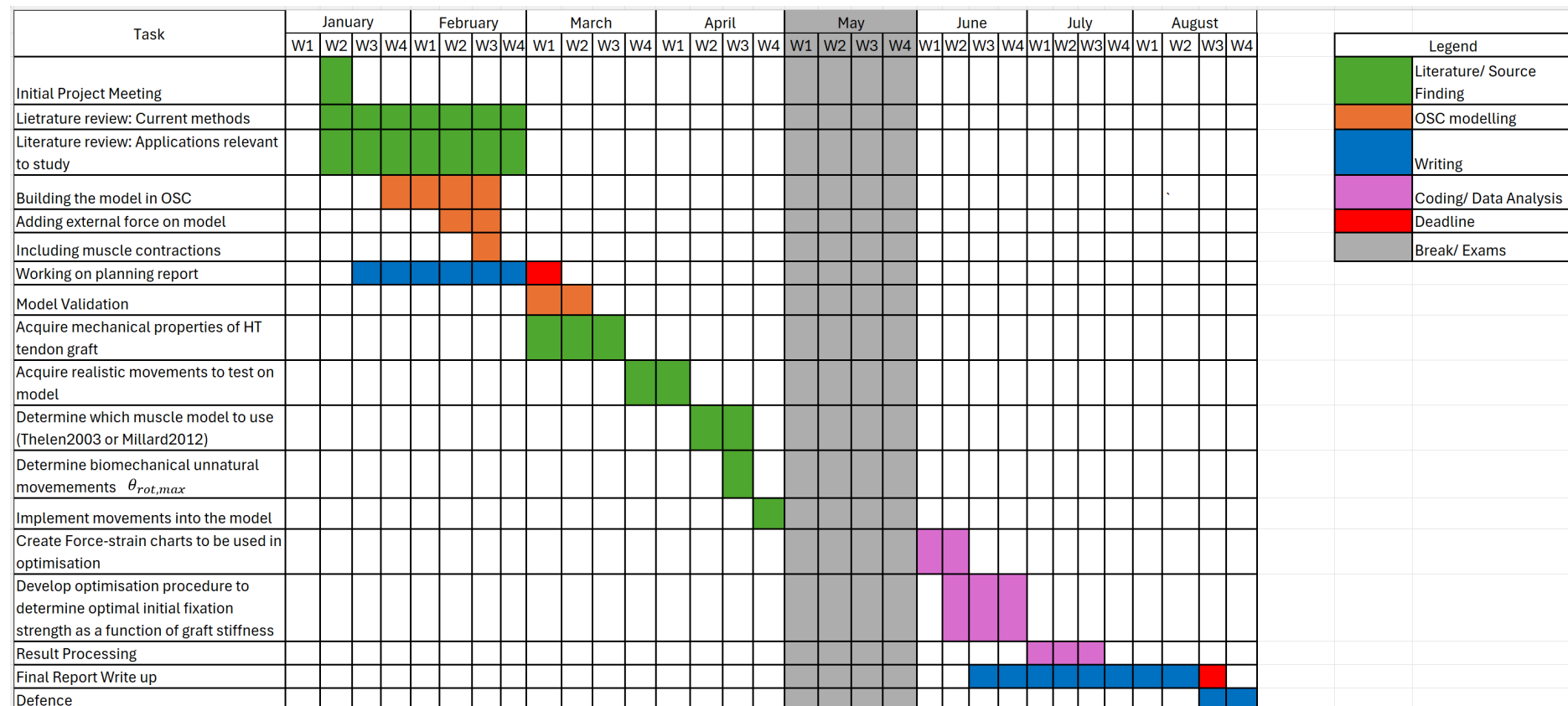


Figure 4.1: Gantt chart of timeline of project

5 Risk Register

Table 5.1: Likelihood and severity matrix for evaluating risk

| | | Severity | | | | |
|------------|---|----------|----|----|----|----|
| | | 1 | 2 | 3 | 4 | 5 |
| Likelihood | 1 | 1 | 2 | 3 | 4 | 5 |
| | 2 | 2 | 4 | 6 | 8 | 10 |
| | 3 | 3 | 6 | 9 | 12 | 15 |
| | 4 | 4 | 8 | 12 | 16 | 20 |
| | 5 | 5 | 10 | 15 | 20 | 25 |

Table 5.2 summarises the biggest risks in the project as well as how they will be dealt with should they appear.

Table 5.2: Risk register table

| Risk | Risk Description | Likelihood | Impact | Risk Level | Mitigation Strategy |
|---|--|------------|--------|------------|---|
| Biological Variability | The material properties of each individual is different, as well as the structure of their body. This could affect the generalisability of the model | 4 | 3 | 12 | This is inherent to computational biomechanics. As we are basing our study on a general model, this is a limitation we should consider. However, it does not alter the validity of our study should we show that tensioning depending on variable stiffness has an effect on knee biomechanics. |
| Starting assumptions are wrong | The model is based on certain assumptions that have been made (for example muscle insertion location). Wrong assumptions will in essence invalidate the whole model. | 2 | 5 | 10 | The model of the lower limbs and the ligaments is taken from a previous validated study. Several studies have used the model ([17]). Any further assumptions made (for instance identifying critical movements to be tested) will have to be cited. |
| Non-convergence of optimisation procedure | The optimisation procedure will determine the optimal tension to apply for a given stiffness. If the optimisation does not converge, that could be a result of overcomplicating the model | 3 | 3 | 9 | The study will look at individual joint rotations independently first before combining them |
| Limited data availability | The mechanical properties of the materials are crucial for the simulation. The most important will be the stiffness of the graft, but also the damping coefficient to be used. If data is limited, then it could hinder the results. | 2 | 4 | 8 | From the literature, it was shown that the tendon graft behaves similarly to the ligament ([27]). Should no data be available, a correct assumption would be to use the default value of the ligament. |
| Data Loss | Computer crash could result in data loss | 1 | 5 | 5 | GitHub repository is being updated consistently |
| Unrealistic knee laxity | Knee can have too many degrees of freedom which can alter the movement in an unrealistic way and invalidate the simulation | 1 | 3 | 3 | Angles will be restricted to what is biomechanically accurate and irrelevant DOF will be removed |

6 Evaluation

6.1 Measures of Success

There are numerous targets the project can achieve for it to be deemed successful. Ideally, the final conclusion of the paper would be assuming a patient graft stiffness K_s , the initial tension of the graft should be $F_0 = \alpha K_s$, where α is some coefficient of proportionality to be determined. Note that F_0 can be used to compute the strain ϵ_0 (see section 3.2.3) and as such we can determine what the initial strain ϵ_0 should be. As the gap between the surfaces (condyles and tibia) is fixed, and the initial strain is determined, the length of the graft to be used L_{use} can be determined using the equation below. L_{use} is the only segment of the graft that is able to produce a force. The rest of the graft ($L_{tot} - L_{use}$) is used to fixate the graft to the bone and for the purpose of this paper will not produce any force.

$$\epsilon_0 = \frac{h_{gap} - L_{use}}{L_{use}}$$

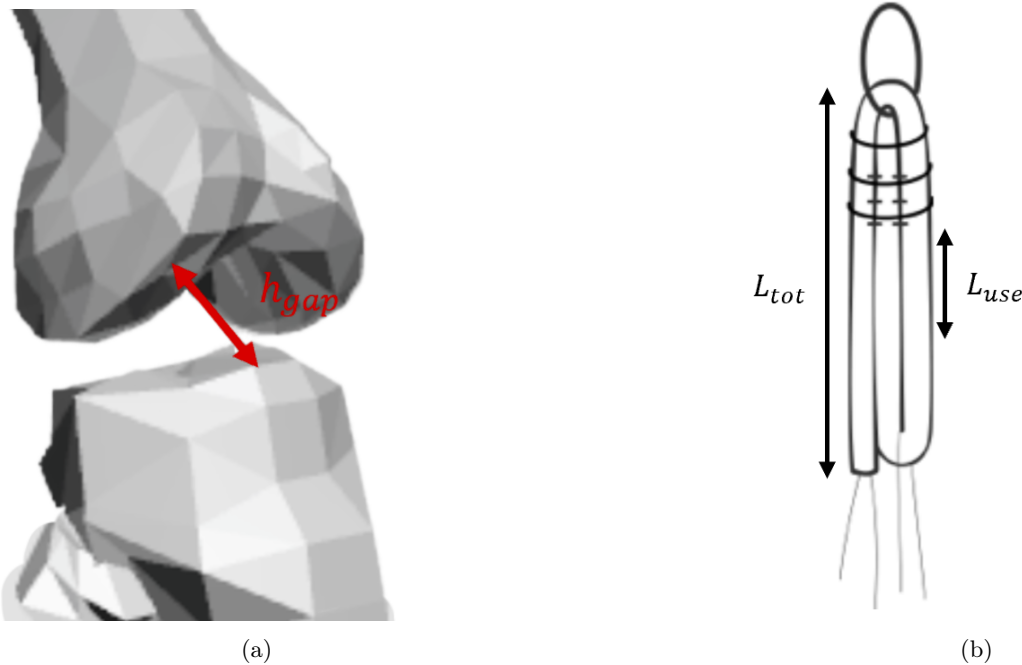


Figure 6.1: (a) Gap between condyles and tibia at 30°, flexion, h_{gap} . (b) Used length of graft, L_{use} , and total length of graft, L_{tot}

However, there are smaller goals that are also indicative that the project was successful. For instance, having a correct model that includes the relevant ligaments as well as their strain is a very realistic goal to achieve. Furthermore, being able to include external forces and analysing how these impact the strains of the ligaments is also a step in the right direction. Finally, including muscle activation allows us to investigate how muscle activation impact the strain of the ligaments. This can yield another research topic, one where we compare the importance of muscle strength in injury prevention.

6.2 Potential Limitations

The study will have limitations that need be considered and addressed. Firstly, the computational model is fixed and the segments cannot be changed. As such, while attempting to create a pipeline where the initial strain can be determined, h_{gap} will be different for each individual. Including different geometries of the bones as well as their different masses is beyond the scope of this paper and should be included in future research. The same argument can be made regarding the ligament stiffness's and muscle forces which are of course individual to each person. This paper will attempt to show that not personalising initial graft tension during ACLR can produce harm and can hinder successful rehabilitation.

Furthermore, different fixation techniques also impact the fixation strength of the graft with the bone [14]. For the purpose of this paper, we will assume that the fixation will not be the cause of graft failure.

Another aspect that is considered is the fluctuation of the structural properties of the ligaments and tendons at different temperatures [29]. These fluctuations will not be considered as it is beyond the scope of this paper and we will assume body temperature throughout the study.

Additionally, when the graft is fixed in the knee, there is a ligamentisation process that is taking place and can last up to a year ([30], [31]) in which the composition and organisation of extra-cellular matrix are adapted to the functions of an active ACL [32]. While the process is not complete, the material properties of the tendon graft are changing and during the first year after ACL reconstruction, the strength and resistance of the graft are only 30% and 50% of the original ACL [30]. The strength of the graft during the rehabilitation stage can be represented using figure 6.2. The time when the graft is weakest will be considered in the paper as well as the graft after the ligamentisation process is completed. This will be done by modifying the stiffness and damping values of the graft.

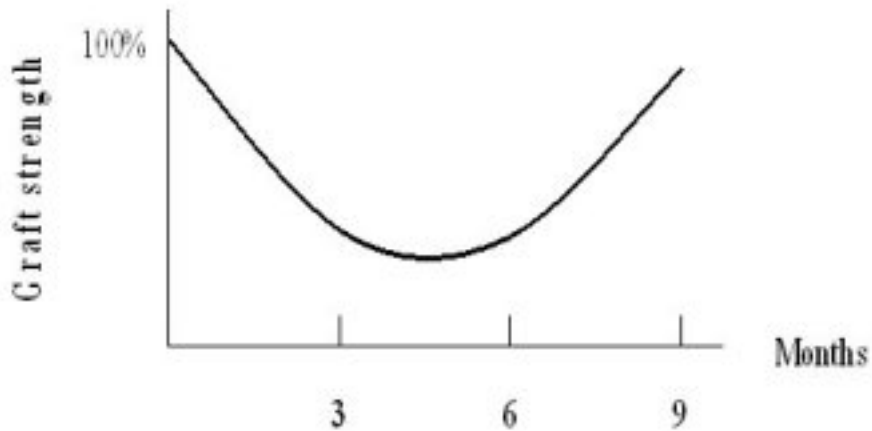


Figure 6.2: Graft strength following surgery [33]

Finally, it is known that muscle atrophy occurs following ACLR surgery [34] [35] however, for the purpose of this study, the muscle properties will be kept the same. This is because it is assumed that the patient will follow a rehabilitation plan that will negate any differences in muscle strength pre and post-surgery. Furthermore, when considering the passive viscoelastic properties of the muscle (i.e. no muscle activation), there is no difference pre and post surgery.

7 Preliminary Results

7.1 Computational Model

The computational model is complete. It is based on a three-dimensional, 23 degree-of-freedom computer model of the human musculoskeletal system. The models feature lower extremity joint definitions adopted from Delp et al. [36], low back joint and anthropometry adopted from Anderson and Pandy et al. [37], and a planar knee model adopted from Yamaguchi and Zajac et al. [38]. Figure 7.1 shows an anterior and posterior view of the model. The model features 92 musculotendon actuators to represent 76 muscles in the lower extremities and torso. The default, unscaled version of the models a subject that is about 1.8 m tall and weighs 75.16 kg. The gracilis semitendinosus will be removed from the model as it will be used for the graft. More details regarding the model's construction can be found in appendix A.

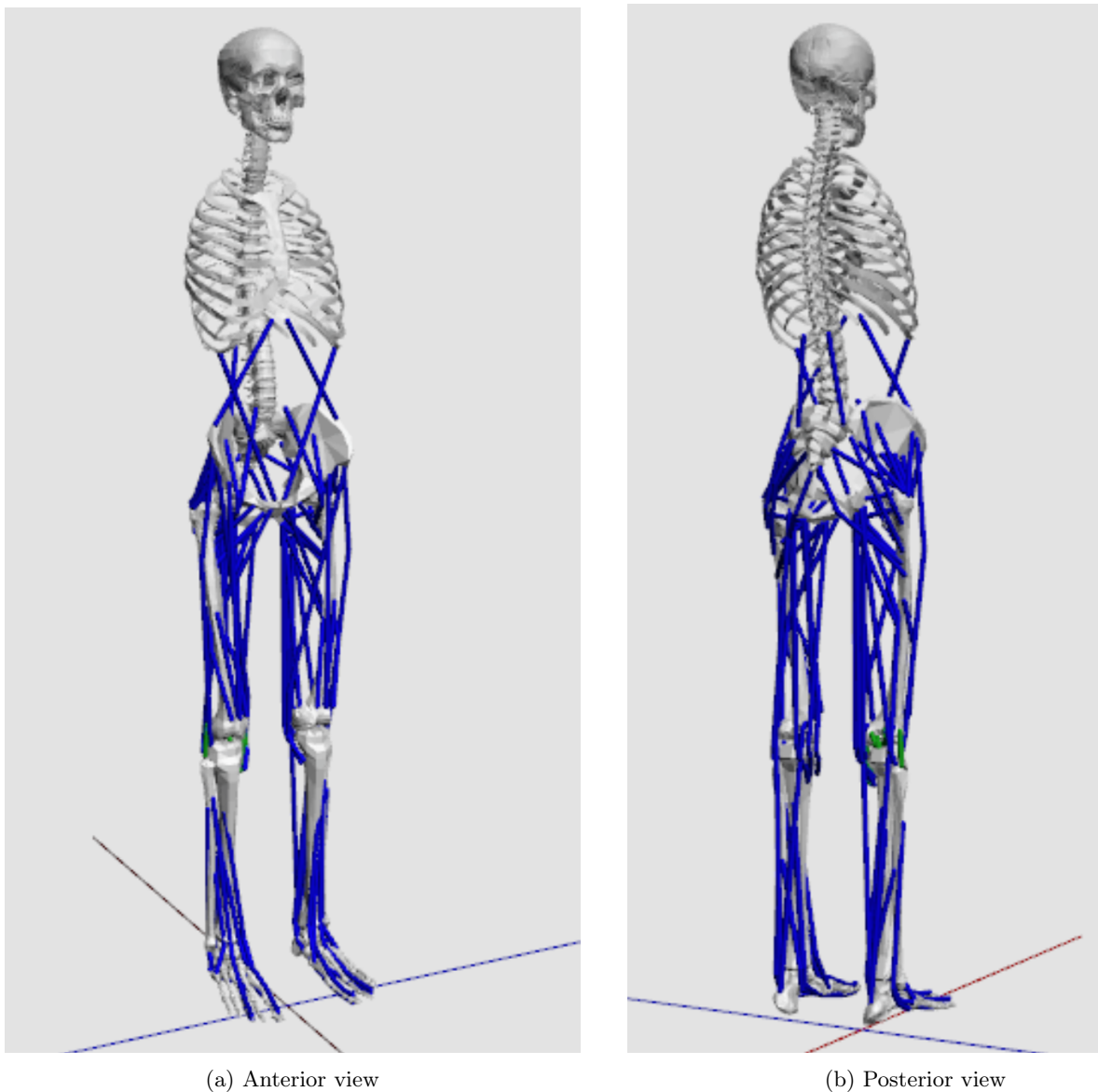
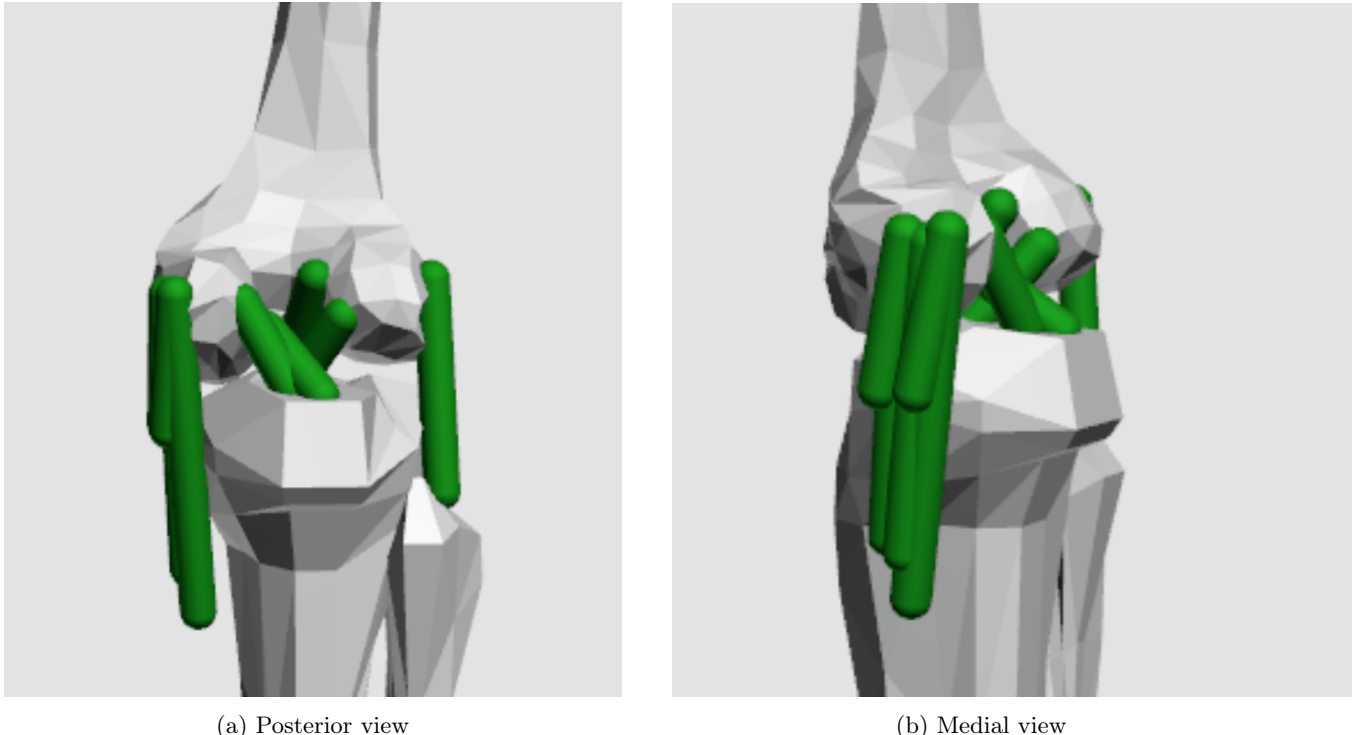


Figure 7.1: Computational model

Additionally, the knee ligaments have also been modelled according to the article by Xu et al. Figure 7.2 shows a posterior and medial view of the knee. Is it to be noted that the patella and the meniscus have not been included. The patella was removed from the model to avoid kinematic constraints (see appendix A).



(a) Posterior view

(b) Medial view

Figure 7.2: Posterior and medial view of the knee ligaments in the model

7.2 Partial Validation of Model Kinematics

As explained in the literature review, the kinematics of the ligaments must be compared with physiological data in order to validate the model. Figure 7.3 shows a similar curve to the LCL strain for varying internal rotation angles of the knee. Figure 7.4 shows the strains of the aACL and pACL published by Xu et al and the strains obtained using the computational model (note flexion in this study is negative).

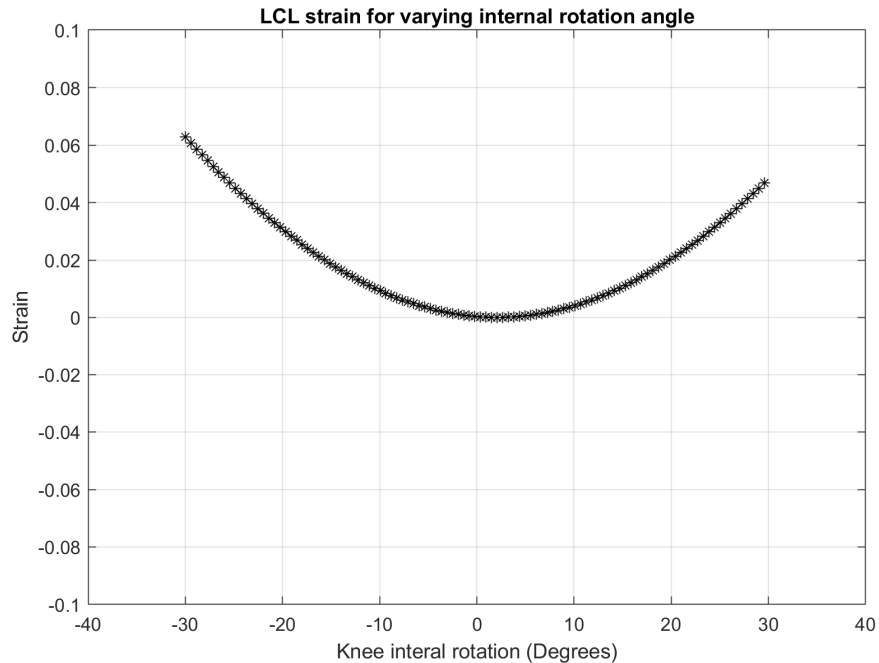


Figure 7.3: LCL strain change by independent knee internal rotation

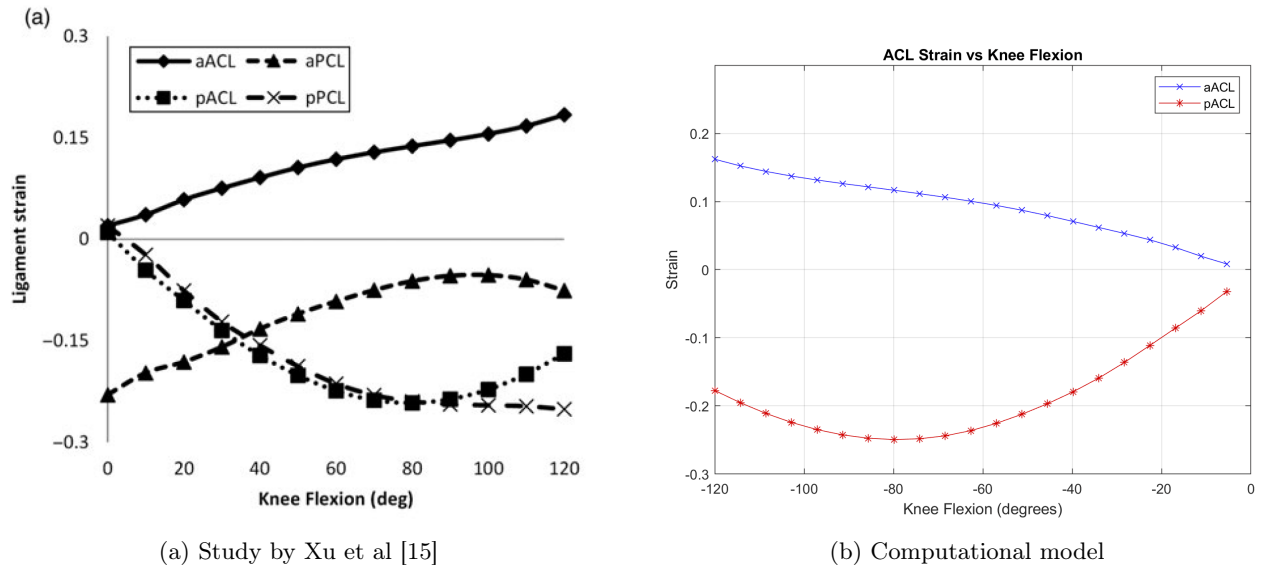


Figure 7.4: Strain of aACL and pACL in study by Xu et al and in current(note flexion in model is negative)

7.3 Including External Force on the model

An external force can now been included in the model. It can be a constant torque or force applied at a particular point of the model.

7.4 Including Muscle Activation on the Model

The muscles in the model can be activated. This will be crucial to analyse how co-contraction of muscles affects the graft initial tension. Figure 7.5 shows the model flexing the knee as a result of the full activation of the long head of the bicep femoris.

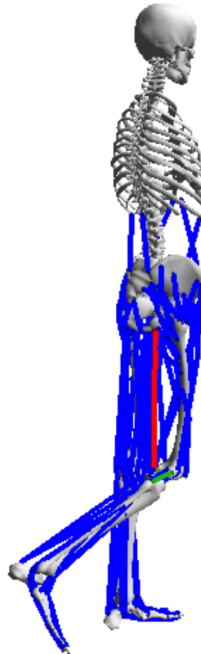


Figure 7.5: Long head bicep femoris activation

7.5 Procedure for Optimisation

A pipeline to determine whether the graft is too loose or too tight has also been developed. This will be explained using two scenarios, one where a desired joint angle needs to be achieved (for instance 60° knee flexion) and one where a specific torque T is applied to the joint. In both cases, we can first start with a force balance on the knee joint for a movement. This can be seen in figure 7.6. For equilibrium we have,

$$\mathbf{T} = \mathbf{r} \times \mathbf{F}_{ACL}$$

where, \mathbf{T} is the torque applied, \mathbf{r} is the location of the insertion of the ACL in the body frame and \mathbf{F}_{ACL} is the force of the ACL.

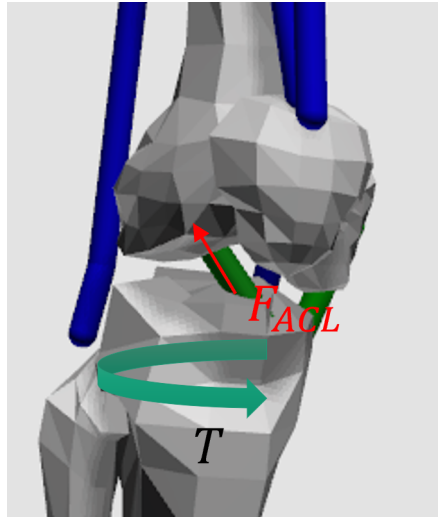


Figure 7.6: Force balance of the knee when a torque is applied

\mathbf{F}_{ACL} is composed of the initial tension force \mathbf{F}_0 and the elastic component as a result of the strain of the ligament $\mathbf{F}_{elastic}$.

$$\mathbf{F}_{ACL} = \mathbf{F}_0 + \mathbf{F}_{elastic}$$

7.5.1 Scenario 1: Desired Joint Angle

When a joint angle is desired there will be a change in length of the ACL to achieve the angle ($\theta \rightarrow \Delta x$). Figure 7.7 is a force-displacement graph of the ACL where when a certain joint angle is desired, the force on the ACL is larger than the yield stress and as such the ACL will fail. Note the change in length of the ACL will be calculated using DIBS (section 3.2.4).

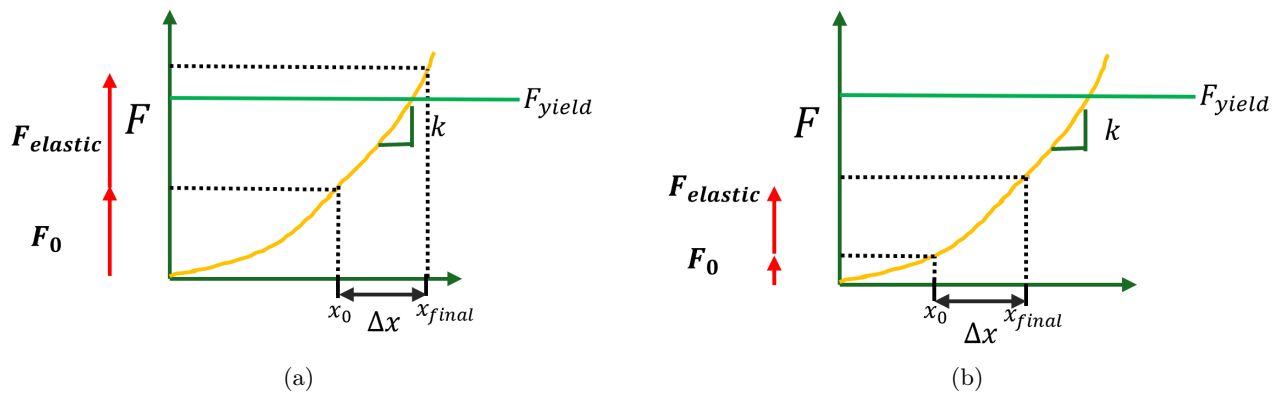


Figure 7.7: Force required to achieve desired joint angle. (a) Graft is too tight resulting in graft failure. (b) After reducing initial tension, desired angle is achieved under graft yield strength. Δx is the same in both as θ is the same

In this scenario, the graft was too tight resulting in joint stiffness and loss of range of motion. The solution here is to reduce the initial tension.

7.5.2 Scenario 2: Desired Torque

For a given torque \mathbf{T} , the ACL must produce a force such that $\mathbf{T} = \mathbf{r} \times \mathbf{F}_{ACL}$. This will cause a change in length of the ACL to produce the necessary amount of force to reach equilibrium. Figure 7.8 shows a force-displacement graph when a given torsion is applied and the joint angle becomes extremely large resulting in unnatural movement that can damage the joint.

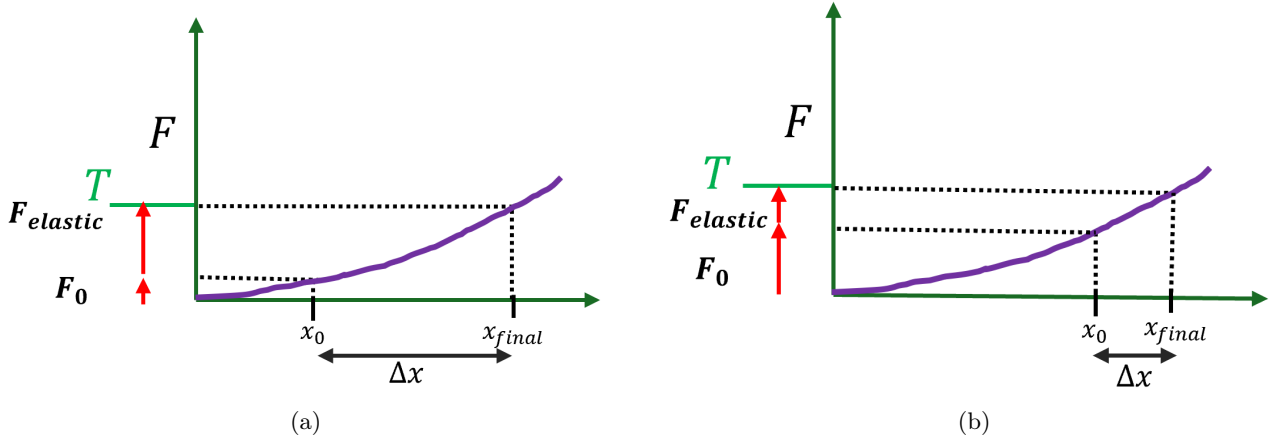


Figure 7.8: Δx required to achieve equilibrium. (a) Graft is too loose resulting in unnatural movement due to extreme joint angle (large Δx). (b) After increasing initial tension, desired tension is achieved with decrease in joint angle. T is the same in both graphs

A solution is thus to increase the graft initial tension to reduce the joint angle required to achieve equilibrium. Using the scenarios above, an optimisation procedure can be designed where the goal will be to find an initial graft tension F_0 that does not result in knee laxity or loss of range of motion. We can set the yield stress of the graft as well as the maximal joint angles that can be considered as safe. Furthermore, including the approximate force required to flex the knee can also be a good indicator whether the graft is too tight or not. For example, if all the hamstring muscles are activated and limited knee extension is achieved (value still to be determined), then we can assume that the graft is too tight. This will also be included in the optimisation procedure.

References

- [1] N. K. Paschos and S. M. Howell, "Anterior cruciate ligament reconstruction: Principles of treatment," *EFORT Open Reviews*, vol. 1, 2016.
- [2] O. Chechik, E. Amar, M. Khashan, R. Lador, G. Eyal, and A. Gold, "An international survey on anterior cruciate ligament reconstruction practices," 2013.
- [3] H. Sheth, A. A. Salunke, R. Barve, and R. Nirke, "Arthroscopic acl reconstruction using fixed suspensory device versus adjustable suspensory device for femoral side graft fixation: What are the outcomes?," *Journal of Clinical Orthopaedics and Trauma*, vol. 10, p. 138–142, Jan. 2019.
- [4] J. Wilde, A. Bedi, and D. W. Altchek, "Revision anterior cruciate ligament reconstruction," *Sports Health: A Multidisciplinary Approach*, vol. 6, p. 504–518, Aug. 2013.
- [5] S. Arneja, M. O. McConkey, K. Mulpuri, P. Chin, M. K. Gilbart, W. D. Regan, and J. M. Leith, "Graft tensioning in anterior cruciate ligament reconstruction: A systematic review of randomized controlled trials," *Arthroscopy: The Journal of Arthroscopic and Related Surgery*, vol. 25, p. 200–207, Feb. 2009.
- [6] S. Yoshiya, M. Kurosaka, K. Ouchi, R. Kuroda, and K. Mizuno, "Graft tension and knee stability after anterior cruciate ligament reconstruction," *Clinical Orthopaedics and Related Research*, vol. 394, p. 154–160, Jan. 2002.
- [7] S. D. Abramowitch, C. D. Papageorgiou, J. D. Withrow, T. W. Gilbert, and S. L.-Y. Woo, "The effect of initial graft tension on the biomechanical properties of a healing acl replacement graft: A study in goats," *Journal of Orthopaedic Research*, vol. 21, no. 4, pp. 708–715, 2003.
- [8] L. Sharma, C. Lou, D. T. Felson, D. D. Dunlop, G. Kirwan-Mellis, K. W. Hayes, D. Weinrach, and T. S. Buchanan, "Laxity in healthy and osteoarthritic knees," *Arthritis and Rheumatism*, vol. 42, p. 861–870, May 1999.
- [9] E. D. Nabors, J. C. Richmond, W. M. Vannah, and O. R. McConville, "Anterior cruciate ligament graft tensioning in full extension," *The American Journal of Sports Medicine*, vol. 23, p. 488–492, July 1995.
- [10] K. L. MARKOLF, D. M. BURCHFIELD, M. M. SHAPIRO, B. R. DAVIS, G. A. M. FINERMAN, and J. L. SLAUTERBECK, "Biomechanical consequences of replacement of the anterior cruciate ligament with a patellar ligament allograft. part i: Insertion of the graft and anterior-posterior testing*," *The Journal of Bone and Joint Surgery*, vol. 78, p. 1720–7, Nov. 1996.
- [11] A. Malige, S. Baghdadi, M. W. Hast, E. C. Schmidt, K. G. Shea, and T. J. Ganley, "Biomechanical properties of common graft choices for anterior cruciate ligament reconstruction: A systematic review," *Clinical Biomechanics*, vol. 95, p. 105636, May 2022.
- [12] J. Suggs, C. Wang, and G. Li, "The effect of graft stiffness on knee joint biomechanics after acl reconstruction—a 3d computational simulation," *Clinical Biomechanics*, vol. 18, p. 35–43, Jan. 2003.
- [13] B. J. O'Neill, F. J. Byrne, K. M. Hirpara, W. F. Brennan, P. E. McHugh, and W. Curtin, "Anterior cruciate ligament graft tensioning. is the maximal sustained one-handed pull technique reproducible?," *BMC Research Notes*, vol. 4, July 2011.
- [14] D. H. Kim, D. R. Wilson, A. T. Hecker, T. M. Jung, and C. H. Brown, "Twisting and braiding reduces the tensile strength and stiffness of human hamstring tendon grafts used for anterior cruciate ligament reconstruction," *The American Journal of Sports Medicine*, vol. 31, p. 861–867, Nov. 2003.
- [15] H. Xu, D. Bloswick, and A. Merryweather, "An improved opensim gait model with multiple degrees of freedom knee joint and knee ligaments," *Computer Methods in Biomechanics and Biomedical Engineering*, vol. 18, p. 1217–1224, Mar. 2014.
- [16] L. Blankevoort, R. Huiskes, and A. de Lange, "Recruitment of knee joint ligaments," *Journal of Biomechanical Engineering*, vol. 113, p. 94–103, Feb. 1991.
- [17] C. Smith, "API: OpenSim::Blankevoort1991Ligament Class Reference — simtk.org." https://simtk.org/api_docs/opensim/api_docs/classOpenSim_1_1Blankevoort1991Ligament.html#details, August 2022. [Accessed 28-02-2024].

- [18] C. Smith, R. Lenhart, J. Kaiser, M. Vignos, and D. Thelen, “Influence of ligament properties on tibiofemoral mechanics in walking,” *Journal of Knee Surgery*, vol. 29, p. 099–106, Sept. 2016.
- [19] M. A. Marra, V. Vanheule, R. Fluit, B. H. F. J. M. Koopman, J. Rasmussen, N. Verdonschot, and M. S. Andersen, “A subject-specific musculoskeletal modeling framework to predict in vivo mechanics of total knee arthroplasty,” *Journal of Biomechanical Engineering*, vol. 137, Feb. 2015.
- [20] S. Razu, H. Jahandar, and T. Guess, “Evaluation of knee ligament mechanics using computational models,” *Journal of Knee Surgery*, vol. 29, p. 126–137, Jan. 2016.
- [21] G. Li, J. Gil, A. Kanamori, and S. L.-Y. Woo, “A validated three-dimensional computational model of a human knee joint,” *Journal of Biomechanical Engineering*, vol. 121, p. 657–662, Dec. 1999.
- [22] A. Ristaniemi, L. Stenroth, S. Mikkonen, and R. Korhonen, “Comparison of elastic, viscoelastic and failure tensile material properties of knee ligaments and patellar tendon,” *Journal of Biomechanics*, vol. 79, p. 31–38, Oct. 2018.
- [23] R. B. Martin, D. B. Burr, N. A. Sharkey, and D. P. Fyhrie, *Mechanical Properties of Ligament and Tendon*, pp. 175–225. New York, NY: Springer New York, 2015.
- [24] J. A. Weiss and J. C. Gardiner, “Computational modeling of ligament mechanics,” *Critical Reviews in Biomedical Engineering*, vol. 29, no. 3, p. 303–371, 2001.
- [25] D. Pioletti, L. Rakotomanana, J.-F. Benvenuti, and P.-F. Leyvraz, “Viscoelastic constitutive law in large deformations,” *Journal of Biomechanics*, vol. 31, p. 753–757, Aug. 1998.
- [26] D. Pioletti, L. Rakotomanana, and P.-F. Leyvraz, “Strain rate effect on the mechanical behavior of the anterior cruciate ligament–bone complex,” *Medical Engineering and Physics*, vol. 21, p. 95–100, Mar. 1999.
- [27] D. Özer Kaya, *Architecture of tendon and ligament and their adaptation to pathological conditions*, p. 115–147. Elsevier, 2020.
- [28] M. Marieswaran, A. Sikidar, A. Goel, D. Joshi, and D. Kalyanasundaram, “An extended opensim knee model for analysis of strains of connective tissues,” *BioMedical Engineering OnLine*, vol. 17, Apr. 2018.
- [29] H. Lee, “Effect of heat and cold on tendon flexibility and force to flex the human knee,” *Medical Science Monitor*, vol. 19, p. 661–667, 2013.
- [30] R. P. A. Janssen and S. U. Scheffler, “Intra-articular remodelling of hamstring tendon grafts after anterior cruciate ligament reconstruction,” *Knee Surgery, Sports Traumatology, Arthroscopy*, vol. 22, p. 2102–2108, Aug. 2013.
- [31] S. Yao, B. S.-C. Fu, and P. S.-H. Yung, “Graft healing after anterior cruciate ligament reconstruction (aclr),” *Asia-Pacific Journal of Sports Medicine, Arthroscopy, Rehabilitation and Technology*, vol. 25, p. 8–15, July 2021.
- [32] S. Yao, P. S. H. Yung, and P. P. Y. Lui, “Tackling the challenges of graft healing after anterior cruciate ligament reconstruction-thinking from the endpoint,” *Front. Bioeng. Biotechnol.*, vol. 9, p. 756930, Dec. 2021.
- [33] I. McDermott, “ACL reconstruction.” <https://sportsortho.co.uk/treatment/acl-reconstruction/>.
- [34] L. K. Lepley, S. M. Davi, J. P. Burland, and A. S. Lepley, “Muscle atrophy after acl injury: Implications for clinical practice,” *Sports Health: A Multidisciplinary Approach*, vol. 12, p. 579–586, Aug. 2020.
- [35] M. Tim-Yun Ong, S.-C. Fu, S.-W. Mok, A. Franco-Obregón, S. Lok-Sze Yam, and P. Shu-Hang Yung, “Persistent quadriceps muscle atrophy after anterior cruciate ligament reconstruction is associated with alterations in exercise-induced myokine production,” *Asia-Pacific Journal of Sports Medicine, Arthroscopy, Rehabilitation and Technology*, vol. 29, p. 35–42, July 2022.
- [36] S. Delp, J. Loan, M. Hoy, F. Zajac, E. Topp, and J. Rosen, “An interactive graphics-based model of the lower extremity to study orthopaedic surgical procedures,” *IEEE Transactions on Biomedical Engineering*, vol. 37, no. 8, p. 757–767, 1990.

- [37] F. C. ANDERSON and M. G. PANDY, “A dynamic optimization solution for vertical jumping in three dimensions,” Computer Methods in Biomechanics and Biomedical Engineering, vol. 2, p. 201–231, Jan. 1999.
- [38] G. T. Yamaguchi and F. E. Zajac, “A planar model of the knee joint to characterize the knee extensor mechanism,” Journal of Biomechanics, vol. 22, p. 1–10, Jan. 1989.

A Further Details Model

Gait 2392 and 2354 Models

Gait 2392 and 2354 Models

The Gait 2392 Model and Gait 2354 Model are three-dimensional, 23 degree-of-freedom computer model of the human musculoskeletal system. The models were created by Darryl Thelen, Univ. of Wisconsin-Madison, and Ajay Seth, Frank C. Anderson, and Scott L. Delp, Stanford University. The models feature lower extremity joint definitions adopted from Delp et al. (1990), low back joint and anthropometry adopted from Anderson and Pandy et al. (1999), and a planar knee model adopted from Yamaguchi and Zajac et al. (1989).

The Gait 2392 model features 92 musculotendon actuators to represent 76 muscles in the lower extremities and torso. For the Gait 2354 model, the number of muscles was reduced by Anderson to improve simulation speed for demonstrations and educational purposes. Seth removed the patella to avoid kinematic constraints; insertions of the quadriceps are handled with moving points in the tibia frame.

The default, unscaled version of the models a subject that is about 1.8 m tall and weighs 75.16 kilograms.

The models can be used and modified in OpenSim, an open source biomechanics simulation application. Some of the uses of the models include:

1. Computing the maximum isometric force and joint moment a muscle can develop at any body position
2. Studying how surgical changes in musculoskeletal geometry (e.g. origin-to-insertion path) and muscle-tendon parameters (e.g. optimal muscle-fiber length and tendon slack length) can affect the moment-generating capacity of the different muscles on the human body
3. Generating muscle drive forward simulations of walking and running to analyze how muscles contribute to motions (e.g. Induced Acceleration Analysis) or how joints are loaded (see Joint Reactions Analysis).

See the sections below for more information about the following components of these models:

- [Gait 2392 and 2354 Models](#)
 - [Accessing the Models](#)
 - [Kinematics](#)
 - [Bone geometry](#)
 - [Joint geometry](#)
 - [Muscle geometry](#)
 - [Dynamics](#)
 - [Inertial properties](#)
 - [Actuators and Other Force-Generating Elements](#)
 - [Associated Publications](#)

Accessing the Models

The musculoskeletal file (.osim), the setting files (.xml), and associated result files (.mot, .sto) for this model are provided free of charge with the OpenSim software for researchers interest in reproducing the result of the simulation. These files can be accessed via the [Models/Gait2392_Simbody or Models/Gait2354_Simbody](#) folder in the OpenSim 3.0 installation directory, and the [example/Gait2392_Simbody or Models/Gait2392_Simbody](#) folder in the OpenSim 2.4.0 installation directory.

Kinematics

Bone geometry

Bones surface data for the pelvis and the thigh are obtained by first marking the surfaces of bones with a mesh of polygons, and then determining the coordinates of the vertices with a three-dimensional digitizer. Data describing the shank and foot bones are adopted from Stredney et al (1982).

Joint geometry

The lower extremity has seven right-body segments: pelvis, femur, patella, tibia/fibula, talus, foot (which includes the calcaneus, navicular, cuboid, cuneiforms, metatarsals), and toes. Reference frames are fixed in each segment.

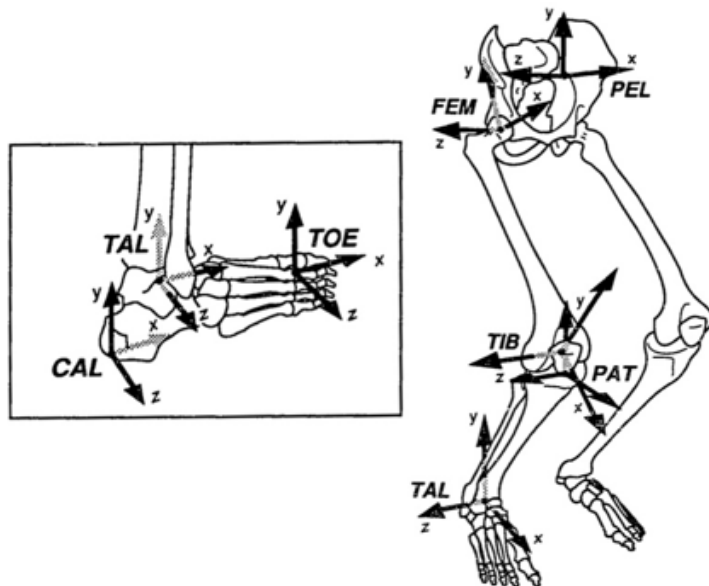


Figure 1 Location of the body-segmental reference frames (Delp et al., 1990).

- **Pelvis:** The pelvic reference frame is fixed at the midpoint of the line connecting the two anterior superior iliac spines
- **Femur:** The femoral frame is fixed at the center of the femoral head
- **Tibia:** The tibial frame is located at the midpoint of the line between the medial and lateral femoral epicondyles
- **Patella:** The patellar frame is located at the most distal point of the patella
- **Talus:** The talar frame is located at the midpoint of the line between the apices of the medial and lateral malleoli
- **Calcaneus:** The calcaneal frame is located at the most interior, lateral point on the posterior surface of the calcaneus
- **Toe:** The toe frame is located at the base of the second metatarsal

Models of the hip, knee, ankle, subtalar, and metatarsophalangeal joints define the relative motions of these segments.

Hip Joint

The hip is characterized as a ball-and-socket joint. The transformation between the pelvic and femoral reference frame is thus determined by successive rotations of the femoral frame about three orthogonal axes fixed in the femoral head.

Knee Joint

Because of its three-bone, multi-ligamentous structure, the knee presents a challenge for the determination of the moment arm of the quadriceps muscles. In order to calculate the extensor moment arm of the knee in a computationally inexpensive way, Yamaguchi et al. (1989) developed a simplified model of the knee. The single-degree-of-freedom model provided by Yamaguchi et al. accounts for the kinematics of both the tibiofemoral joint and the patellofemoral joint in the sagittal plane as well as the patellar levering mechanism. Delp et al. adopted this planar knee model and specified the transformations between the femoral, tibial, and patellar reference frames as functions of the knee angle. Figure 2 illustrates how the planar knee model is adopted in the Delp model of lower limb extremity (1990). In the Delp model, the femoral condyles are represented as ellipses, and the tibial plateau is represented as a line segment. The transformation from the femoral reference frame to the tibial reference frame is specified such that the femoral condyles remain in contact with the tibial plateau throughout the range of knee motion. The tibiofemoral contact point depends on the knee angle and is specified according to data reported by Nisell et al. (1986).

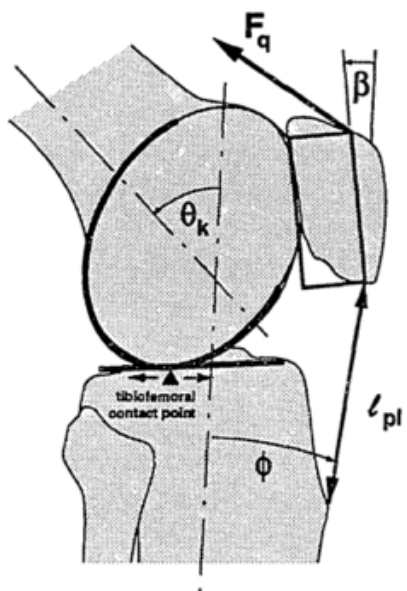


Figure 2: Geometry for determining knee moments and kinematics in the sagittal plane in the Delp model (Delp et al., 1990)

Ajay Seth adapted the Delp model, removing the patella to avoid kinematic constraints. In the Gait 2392 and Gait 2354 models, the insertions of the quadriceps on the tibia are modeled as moving points in the tibial frame.

Ankle, subtalar, and metatarsophalangeal joints

The ankle, subtalar, and metatarsophalangeal joints are modeled as frictionless revolute joints (as seen in **Figure 3**).

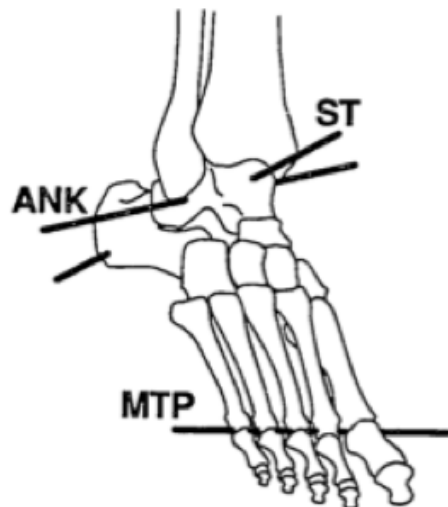


Figure 3. The ankle, subtalar, and metatarsophalangeal joints are modeled as revolute joints with axes oriented as shown. (Delp et al., 1990)

The location and orientation of the axes for each of the joints are modeled after the descriptions provided by Inman (1976), with one modification. When displayed, the axes produce realistic motion of the ankle and subtalar joints (i.e. the bone surface models do not collide or disarticulate), but exhibit unrealistic motion of the metatarsophalangeal joint (i.e. the phalanges separate from the metatarsals). To fix this problem, the metatarsophalangeal axis is rotated by -8 degree on a right-handed vertical axis to minimize disarticulation of the joint.

Muscle geometry

The paths (i.e. the lines of action) of the muscle-tendon actuators in the lower extremity portion of the model are defined based on the anatomical landmarks on the bone surface models. Each muscle-tendon path is represented by a series of line segments. In some cases, for example the soleus, origin and insertion landmarks are sufficient for describing the muscle path. In other cases, where muscle wraps over bone or is constrained by retinacula, intermediate via points are introduced to represent the muscle path more accurately. The number of via points activated for the muscle can depend on body position. For example, because the quadriceps tendon wraps over the distal femur when the knee is flexed beyond 80 degrees, additional via points, also known as "wrapping points," are defined for the knee flexion angles greater than 80 degrees so that the quadriceps tendon can wrap over the bone, instead of passing through it, in that range of knee motion.

Despite the effort to define accurate muscle paths in the lower extremity, there are some muscles that pass through the bones or deeper muscles with extreme hip flexion and extension, and thus yield unrealistic moment arms. Specifically, GMAX3 (the most interior of the gluteus maximus) passes through the ischial tuberosity beyond 60 degree of hip flexion. GMAX1 and GMAX2 (the superior and the middle components of the gluteus maximus) pass through the deeper muscles beyond 80 degree of hip flexion.

For details about what muscles are included in each of the model, refer to the following PDF: [Gait 2392 vs. Gait 2354.pdf](#)

Dynamics

Inertial properties

The inertial parameters for the body segments in the model are adapted from a 10-segment, 23 degree-of-freedom model developed by Frank C. Anderson and Marcus G. Pandy (1999). In the Anderson and Pandy model, mass and inertial properties for all segments, except the hindfeet and toes, are based on average anthropometric data obtained from five subjects (age 26 +/- 3 years, height 177 +/- 3 cm, and weight 70.1 +/- 7.8 kg). All data are recorded according to the method described by McConville et al. (1980). The lengths of the body segments are taken from the Delp model (1990).

For the hindfoot and toes, the mass, position of the center of mass, and moments of inertia are found by representing the volume of each segment by a set of interconnected vertices, the coordinates of which are derived from measuring the surface of a size-10 tennis shoe. Assuming a uniform density of 1.1 g /cm³ for the feet, the density is numerically integrated over the volume of each segment to find the mass.

All inertial parameters for the model are scaled by a factor of 1.05626 from those reported by Anderson and Pandy (1999). **Table 2** summarizes the mass and moments of inertia for each body segment in the Gait 2392 Model.

Table 2: Inertial parameters for the body segments included in the model

| Body segment | Mass (kg) | Moments of inertia | | |
|-----------------|-----------|--------------------|------------|------------|
| | | xx | yy | zz |
| Torso | 34.2366 | 1.4745 | 0.7555 | 1.4314 |
| Pelvis | 11.777 | 0.1028 | 0.0871 | 0.0579 |
| Right femur | 9.3014 | 0.1339 | 0.0351 | 0.1412 |
| Right tibia | 3.7075 | 0.0504 | 0.0051 | 0.0511 |
| Right patella | 0.0862 | 0.00000287 | 0.00001311 | 0.00001311 |
| Right talus | 0.1000 | 0.0010 | 0.0010 | 0.0010 |
| Right calcaneus | 1.250 | 0.0014 | 0.0039 | 0.0041 |
| Right toe | 0.2166 | 0.0001 | 0.0002 | 0.0010 |
| Left femur | 9.3014 | 0.1339 | 0.0351 | 0.1412 |
| Left tibia | 3.7075 | 0.0504 | 0.0051 | 0.0511 |
| Left patella | 0.0862 | 0.00000287 | 0.00001311 | 0.00001311 |
| Left talus | 0.1000 | 0.0010 | 0.0010 | 0.0010 |
| Left calcaneus | 1.250 | 0.0014 | 0.0039 | 0.0041 |
| Left toe | 0.2166 | 0.0001 | 0.0002 | 0.0010 |

Actuators and Other Force-Generating Elements

Peak isometric force

In the original lower limb model developed by Delp et al. (1990), values for the muscle-tendon parameters are determined with a procedure similar to that used by Hoy et al. (1990). Values for muscle physiological cross-sectional area (PCSA), which determine the peak isometric force, are taken from Friederich et al. (1990) and Wickiewicz (1983). Because the measurements reported by Friederich et al. (1990) [25 N·m²] are obtained from experiments on young cadavers, and those reported by Wickiewicz et al. (1983) [61 N·m²] are obtained from experiments on elderly cadavers, a factor that is larger than the "specific tension" reported by Spector et al. (1980) [23 N·m²] is used to scale the PCSA values from the elderly cadavers.

While constructing the Gait 2392 Model from the original Delp model, Anderson noticed that the muscle strengths in the Delp model were still weak compared to the experimental results from Anderson and Pandy (1999) and Carhart (2000) on healthy, living subjects. To better match the strength of the Delp model to the joint torque-angle relationships measured in living subjects, additional strength scaling was employed. Despite efforts to keep the scaling factor consistent across all muscles, a different scaling factor is needed for bi-articular muscles because they span two joints. In many cases, the muscle strength parameters from Anderson and Pandy are used instead, as they are more physiologically accurate. For details, refer to the following PDF of the maximum isometric muscle forces from Gait2392/Gait2354, Delp1990, and Carhart2000, along with the scale factors: [MuscleMaxIsometricForces.pdf](#)

Optimal fiber length and pennation angle

For most muscles, values for the optimal fiber length and pennation angle are taken from Wickiewicz et al. (1983). The fiber lengths reported are scaled by a factor 2.8/2.2, which is the ratio of the sarcomere length at which muscle fibers develop peak force based on the sliding filament theory of muscle contraction (2.8 micrometers) to the sarcomere length measured by Wickiewicz et al. (2.2 micrometers).

For muscles not reported by Wickiewicz et al., the muscle-fiber length and pennation angles measured by Friederich et al. (1990) in the anatomical position are used instead.

Associated Publications

Publications specifying how the kinematic and dynamic properties of the model are defined:

Delp, S.L., Loan, J.P., Hoy, M.G., Zajac, F.E., Topp E.L., Rosen, J.M.: An interactive graphics-based model of the lower extremity to study orthopaedic surgical procedures, IEEE Transactions on Biomedical Engineering, vol. 37, pp. 757-767, 1990. ([Download PDF](#))

Yamaguchi G.T., Zajac F.E.: A planar model of the knee joint to characterize the knee extensor mechanism." J . Biomedcl7. vol. 21. pp. 1-10. 1989. ([Download PDF](#))

Anderson F.C., Pandy M.G.: A dynamic optimization solution for vertical jumping in three dimensions. Computer Methods in Biomechanics and Biomedical Engineering 2:201-231, 1999. ([Download PDF](#))

Anderson F.C., Pandy M.G.: Dynamic optimization of human walking. Journal of Biomechanical Engineering 123:381-390, 2001. ([Download PDF](#))

Carhart, M. R. "Biomechanical Analysis of Compensatory Stepping: Implications for Paraplegics Standing Via FNS," Ph.D Dissertation, Arizona State University, 2000.

Publications supplying anatomical data for the model:

Stredney, D. L. "The representation of anatomical structures through computer animation for scientific, educational and artistic applications," Master Thesis, The Ohio State University, 1982.

Inman, V.T. The Joints of the Ankle. Baltimore: Williams & Wilkins, 1976.

Carhart, M. R. "Biomechanical Analysis of Compensatory Stepping: Implications for Paraplegics Standing Via FNS," Ph.D Dissertation, Arizona State University, 2000.

Friederich, J.A. and Brand, R.A. "Muscle fiber architecture in the human lower limb," J. Biomech., vol. 23, pp. 91-95, 1990.

Wickiewicz, T. L., Roy, R. R., Powell, P. L., and Edgerton, V. R., "Muscle architecture of the human lower limb," Clin. Orthop. Rei. Res., vol. 179, pp. 275-283, 1983.

Hoy, M. G., Zajac, F. E., and Gordon, M. E., "A musculoskeletal model of the human lower extremity: the effect of muscle, tendon, and moment arm on the moment-angle relationship of musculotendon actuators at the hip, knee, and ankle," J. Biomech., vol. 23, pp. 157-169, 1990.